

Glycosylation facilitates transdermal transport of macromolecules

Christopher J. Pino^a, Jordan U. Gutterman^b, Daniel Vonwil^c, Samir Mitragotri^d, and V. Prasad Shastri^{a,c,1}

^aDepartment of Biomedical Engineering, Vanderbilt University, Nashville, TN 37232; ^bDepartment of Molecular Therapeutics, M. D. Anderson Cancer Center, Houston, TX 77030; ^cInstitute for Macromolecular Chemistry and Bioss - Center for Biological Signalling Studies, University of Freiburg, D-79104 Freiburg, Germany; and ^dDepartment of Chemical Engineering and Center for Bioengineering, University of California, Santa Barbara, CA 93106

Edited* by Robert Langer, Massachusetts Institute of Technology, Cambridge, MA, and approved October 30, 2012 (received for review January 18, 2012)

Stratum corneum, the outermost layer of skin, allows transport of only low-molecular weight (<500) lipophilic solutes. Here, we report a surprising finding that avicins (Avs), a family of naturally occurring glycosylated triterpenes with a molecular weight > 2,000, exhibit skin permeabilities comparable to those of small hydrophobic molecules, such as estradiol. Systematic fragmentation of the Av molecule shows that deletion of the outer monoterpene results in a 62% reduction in permeability, suggesting an important role for this motif in skin permeation. Further removal of the tetrasaccharide residue results in a further reduction of permeability by 79%. These results, taken in sum, imply that synergistic effects involving both hydrophobic and hydrophilic residues may hold the key in facilitating translocation of Avs across skin lipids. In addition to exhibiting high permeability, Avs provided moderate enhancements of skin permeability of estradiol and polysaccharides, including dextran and inulin but not polyethylene glycol.

chemical penetration enhancers | hydrophilic-lipophilic balance | saponins | amphiphilic

The outermost layer of the skin, the stratum corneum (SC), comprises densely packed lipids, which form a formidable barrier to the movement of macromolecules (1). The structural and physicochemical characteristics of the SC lipids favor the transport of only hydrophobic molecules and exhibit a strong dependence on size, such that permeation of molecules larger than molecular weight (MW) of 500 is practically negligible (2, 3). These limitations have led to the development of strategies to improve skin permeability of drugs using physical methods, such as iontophoresis (4), sonophoresis (5), electroporation (6), jet injectors (7), and microneedles (8), as well as chemical methods that alter the skin properties (9).

Unlike the penetration pathways of small hydrophobic molecules, which have been well studied (10–12) and accurately modeled (2, 13, 14), penetration of hydrophilic macromolecules across the skin remains poorly understood. Certain peptides have been shown to exhibit adequate skin penetration despite their large size. For example, arginine heptamers have been shown to penetrate across intact skin and induce permeation of a macromolecule, cyclosporine, when conjugated to it (15). Peptides discovered using phage display have also been shown to penetrate intact skin and facilitate delivery of macromolecules, including insulin, and siRNA (16–18). Some studies have also reported on penetration of certain types of nanoparticles across the SC of intact skin (19). In general, however, the extent and pathways of penetration of large solutes across the skin remain unclear.

Here, we study the penetration of a group of macromolecules, avicins (Avs) that are extracted from the desert plan *Acacia victoriae* (20). Avs belong to a family of saponins, which are amphiphilic natural products from a plant origin that possess a characteristic chemical structure of lipophilic triterpenes and hydrophilic sugar residues (Fig. 1). Avs have been shown to possess antibacterial (21) and anti-inflammatory properties (22). In addition, their ability to induce apoptosis through disruption of mitochondria has led to their evaluation as antineoplastic agents (23). Avicin D (AvD) and avicin G (AvG), the two most prevalent isoforms of

Avs, have molecular weights of 2,082 and 2,066, respectively (20). We report herein that the unique chemical structure of Avs enables them to traverse the SC barrier despite their large size, and furthermore to provide enhancement of other coadministered solutes. Using AvG as a model compound, we also elucidate the potential structural elements that might play a role in the transport of large molecules across the SC.

Results

Avs Exhibit Percutaneous Absorption and Transport. Full-thickness porcine skin was used to study permeation due to the resemblance of its properties to human skin (24–26). ¹²⁵I-labeled AvD and AvG exhibited significant percutaneous transport across intact porcine skin. After 24 h, 0.9 to ~2% of the applied dose of AvD and AvG was transported across the SC and into the receiver compartment. Calculated skin permeabilities of Avs range from 1–1.6 × 10⁻³ cm/h, which are comparable to those of estradiol (2.3 × 10⁻³ cm/h), a small lipophilic molecule with excellent transdermal transport characteristics (Table 1). A comparison of the time course of transport of Avs with estradiol reveals a steady-state flux that is quite comparable to that of estradiol (Fig. 2). Over the course of the experiment, 14% of AvD ($\chi_{Avs,skin}$; details are provided in *SI Materials and Methods*) was found to localize in the skin when the donor concentration was maintained at a steady level of 1 mg/mL. Interestingly, SC-water partitioning experiments performed separately indicated that 16 ± 4% of Avs accumulate within the SC of the same area as that used in the permeation experiments, suggesting that under steady state, the Avs localize primarily in the SC and localization in the epidermis or other skin substructures may be minimal.

Octanol-Water and SC-Water Partition Coefficient of Avs. To place the measured skin permeability of Avs in the context of known pathways of transdermal transport, the octanol-water partition coefficient ($K_{o/w}$) and SC-water partition coefficient ($K_{SC/w}$) of AvD were measured (Table 2). These studies indicated that AvD is a moderately lipophilic solute and the two partition coefficients are comparable ($K_{o/w} = 8.22 \pm 0.79$ and $K_{SC/w} = 5.20 \pm 0.72$). These data suggest that Avs have an affinity for the hydrophobic environments of the SC despite possessing several sugar residues, which would otherwise render a hydrophilic nature to the Avs.

Differential Scanning Calorimetric Analysis of Avs-Treated Human Skin. The diversity in chemical structural moieties in the Av molecule can lead to multiple avenues of interactions with the various SC lipid components. To investigate this issue, differential scanning calorimetric (DSC) analysis was carried out on heat-

Author contributions: C.J.P., J.U.G., S.M., and V.P.S. designed research; C.J.P., D.V., and V.P.S. performed research; C.J.P., S.M., and V.P.S. analyzed data; J.U.G. provided avicins; D.V. performed the pig skin isolation; and C.J.P., J.U.G., S.M., and V.P.S. wrote the paper.

The authors declare no conflict of interest.

*This Direct Submission article had a prearranged editor.

¹To whom correspondence should be addressed. E-mail: prasad.shastri@gmail.com.

This article contains supporting information online at www.pnas.org/lookup/suppl/doi:10.1073/pnas.1200942109/-DCSupplemental.

Table 2. Octanol-water and SC-water partition coefficients of AvD (n = 3)

	Partition coefficient (K)	Log(K)
Octanol-water (o/w)	8.22 ± 0.79	0.91 ± 0.04
Octanol-SC (sc/water)	5.20 ± 0.72	0.71 ± 0.06

to 70% (Table S2). Because Avs appear to exhibit affinity and interactions with SC lipids, it was theorized that Avs could potentially serve as chemical penetration enhancers (CPEs) to an extent. The effect of Avs on skin permeability of several low- and high-molecular solutes was also assessed, including estradiol, dextran (MW ~ 3,500), inulin (MW ~ 5,000), and polyethylene glycol (PEG; MW ~ 3,400). Both AvD and AvG induced an approximately twofold increase in permeability of estradiol and over a threefold increase in cumulative delivery at the end of 24 h (Fig. 3 and Table 4). AvD and AvG induced a moderate enhancement of inulin and dextran permeability (1.4- to 1.8-fold), whereas no significant effect on the permeability of PEG was found (Table 5 and Fig. S1).

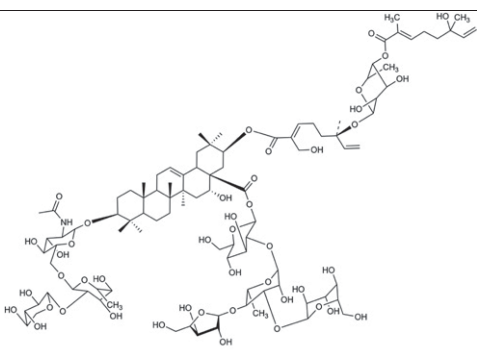
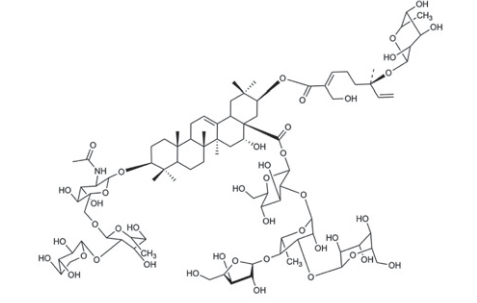
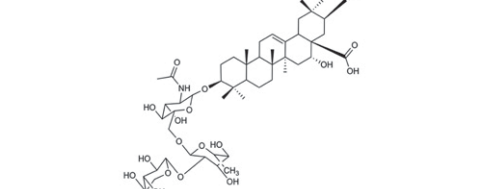
Discussion

The high permeation of AvD and AvG across the SC barrier without the aid of mechanical or chemical enhancement is counterintuitive, given their high molecular weight (>2,000) and water

solubility (Fig. 2). Permeation characteristics of AvD and AvG, such as lag time and steady-state flux, are favorable compared with estradiol, a small hydrophobic molecule (Fig. 3 and Table 1). Permeation of Avs is unlikely to be explained based on classic permeation mechanisms or potential artifacts of the experimental system (details are provided in *SI Mechanism of Penetration of Avicins*). Although the cumulative mass delivered over a 24-h period is potentially adequate to impose, at the site of application, some of the therapeutic effects identified for Avs (22), the finding that F094, which is rich in Avs, enhances the permeability of both Av G and AvD suggests that Avs may be additionally capable of “self-enhancement.” Such a property has been previously observed for some molecules, such as ibuprofen (29).

Avs, despite having appreciable water solubility, exhibited a significant $K_{o/w}$ of 8.22 ± 0.79 (Table 2), suggesting their ability to interact with the SC lipids. DSC studies also provide further evidence for the interactions of Avs with skin lipid components, perhaps even with some degree of specificity. Human SC treated with Avs exhibits a marked absence of thermal transitions in region II (51–55 °C), which have been attributed to lipids that are covalently bound to the proteins of the corneocyte (27, 28). This suggests that Avs potentially interact and associate with lipids around the corneocyte. At the same time, the appearance of the transitions from 90–95 °C, which are otherwise absent in untreated skin, may indicate the presence of new structures associated with Avs and lipids. Because it has been shown that the

Table 3. Fragmented AvG transport across full-thickness pig skin (n = 3)

Donor compartment	Structure	MM, Da	Permeability, cm/h	Reduction in transport
AvG		2,066	1.66 ± 0.73 × 10 ⁻³	NA
Weak-base fragment		1,899	6.21 ± 1.67* × 10 ⁻⁴	62%
Strong-base fragment		969	3.24 ± 1.23* × 10 ⁻⁴	79%

Avs were fragmented as described using weak-base and strong-base hydrolysis and then labeled with ¹²⁵I. The average ± SD is reported. Both weak-base and strong-base fragments were significantly less permeable than AvG, despite their lower molecular weight (AvG vs. weak-base fragment, P < 0.1; AvG vs. strong-base fragment, P < 0.05). NA, not applicable.

*Statistically significant values.

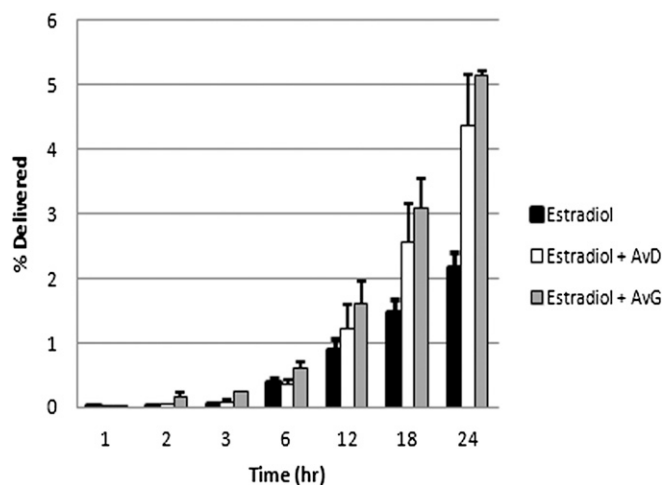


Fig. 3. Estradiol transport in presence of AvD and AvG. The data are presented as the average percentage delivered \pm SD of the donor concentration ($n = 9$). Estradiol cumulative delivery in the presence of AvD and AvG is significantly enhanced ($P < 0.1$) in comparison to estradiol by itself, suggesting a potential role for Avs as CPEs.

hydration state of the SC does not have an impact on the thermal transitions in lipids (28), the observed changes in lipid transitions cannot be attributed to hydration. The similarity of the behavior of untreated and Av-treated skin in region I suggests that Avs do not interact with bulk lipids (alkyl lipids) in the SC, and this is consistent with the observations that the electrical conductivity of the SC before and after Av treatment is virtually unchanged. Nevertheless, one cannot rule out temporary changes to skin barrier properties during the exposure.

The high permeability of Avs could potentially be attributed to their surfactant-like properties, and it is possible that a combination of highly hydrophobic and permeable triterpene core connected with saccharide units that are capable of permeating the skin on their own could be responsible for the unusual permeation properties of Avs (details are provided in *SI Mechanism of Penetration of Avicin*). The small outer glycosylated MT was found to be essential for transport across SC, because the removal of this fragment alone resulted in a 62% reduction in cumulative transport (Table 3). Further removal of sugar residues (except NAG trisaccharide) resulted in an additional 17% (79% overall) reduction in transport. Although the cumulative mass transport of AvG and AvD was similar after 24 h (Fig. 2), they exhibit significantly different lag phases (Table 1). Interestingly, AvD

Table 4. Estradiol transport across full-thickness pig skin in presence of AvD and AvG ($n = 9$)

Donor compartment	Permeability $\times 10^{-3}$, cm/h	Lag time, h	Enhancement factor
Estradiol	2.27 ± 0.48	4.96 ± 2.75	NA
Estradiol + 1 mg/mL AvD	$4.29 \pm 1.26^*$	5.93 ± 2.38	1.93 ± 0.50
Estradiol + 1 mg/mL AvG	$4.19 \pm 0.63^*$	5.43 ± 2.05	1.89 ± 0.65

³H estradiol (saturated solution in PBS with radioactive tracer) was used for the transport studies. The enhancement factor is a comparison measure within each experiment, and it is the ratio of the permeability of estradiol in presence of Avs to its native permeability across SC. The average \pm SD is reported. Estradiol applied with AvD or AvG was significantly more permeable than estradiol applied alone. Differences in lag time were not significant. NA, not applicable.

* $P < 0.1$.

and AvG differ from one another only at the outer MT residue (Fig. 1), providing further compelling evidence for the key role of this moiety in interactions with lipids. The presence of a hydroxyl-methyl group in AvD could promote interactions with the lipid polar head groups, facilitating intercalation into the lipids. This is consistent with the observation that AvD, which has a methyl group in the outer MT moiety, in fact, exhibits a shorter lag time (~ 2 h) in comparison to AvG. When the permeability of the fragmented Avs is taken in sum with percutaneous absorption and transport data (Fig. 2 and Table 3), it is clear that the overall hydrophilic-lipophilic balance (HLB) within the Av molecule may be very important in achieving appreciable mobility through lipid bilayers, because the removal of the hydrophilic glycosylated side chains, which should have an impact on HLB, diminishes the permeability. This suggests that glycosylation may play a critical role in conferring permeability to the Avs through lipid structures. Interestingly, the $\log-K_{o/w}$ for AvD (0.91 ± 0.04) compares well with the $\log-K_{o/w}$ values reported from some terpenoids, which are around 1.18 (30). This provides further evidence in support of the proposed mechanism involving the interactions of the outer MT residue with SC lipids.

In addition to their potential therapeutic properties, Avs present an opportunity to understand the significance of molecular structure in skin permeation. Based on the evidence that Avs interact with the lipids associated with the corneocyte envelope, we postulate that Avs can disrupt lipid organization, thereby enhancing local diffusion, facilitating lateral diffusion, and allowing entry into the corneocytes. The ability of Avs to enhance estradiol permeability (approximately twofold) and cumulative delivery (approximately threefold) implies that the interactions of Avs with lipids may alter the physicochemical characteristics of lipids. This can alter the solvation characteristics of these lipid regions, and hence the partitioning of small-molecular-weight solutes, and this needs to be investigated in future studies. To gain insights into the potential role of Avs in altering the thermodynamic activity of estradiol in the donor compartment, preliminary studies on the partitioning of estradiol from water into isopropylmyristate (IPM) ($K_{IPM/w}$) in the presence of Av-rich extract F094 was studied (Table S3). It was observed that the $K_{IPM/w}$ of estradiol is marginally affected at low Av concentrations of 1 mg/mL; however, at 5 mg/mL F094, a moderate enhancement of around 74% is observed. Interestingly, at higher concentrations of F094 (>10 mg/mL), a slight negative enhancement was noted, suggesting that Avs have the potential to increase the solubility of hydrophobic solutes in water. Although these trends are not statistically significant, they suggest that Avs may alter the thermodynamic activity of drugs through a combination of entropic and solubilization effects, and this needs further study. When analyzed in the context of the $K_{IPM/w}$ data, the observation that the lag phase of estradiol is increased in the presence of Avs suggests some fundamental changes to the transport pathways within the skin, which also requires further investigation.

Based on the observation that Av mixtures (F094) enhance AvG and AvD transport, studies were carried out to ascertain if Avs can indeed facilitate the transport of other water-soluble macromolecules of similar molecular weight. The choice of these macromolecules was based on structure and molecular weight considerations, such that the role of glycosylation (dextran vs. PEG) and molecular weight (dextran vs. inulin) on transdermal transport in presence of Avs may be discerned. Although both inulin and dextran exhibit permeability enhancement in presence of Avs (AvD $\sim 170\%$, AvG $\sim 140\%$; Table 4), PEG, a water-soluble polymer that does not possess sugar residues along the backbone, did not exhibit an enhancement (Table 5 and Fig. S1). These results, in conjunction with the fragmentation studies, suggest a significant role for the sugar residues in Av-mediated transport across the SC. It is important to note that the enhancement in estradiol, dextran, and inulin permeability is modest, and that

Table 5. Transport of macromolecules across full-thickness pigskin in presence of Av D and AvG

Donor compartment	Permeability, cm/h	Enhancement factor
Inulin	$2.21 \pm 0.55 \times 10^{-5}$	NA
Inulin with 1 mg/mL AvD	$3.92 \pm 0.89^* \times 10^{-5}$	1.77 ± 0.40
Inulin with 1 mg/mL AvG	$3.12 \pm 0.43^* \times 10^{-5}$	1.41 ± 0.20
Dextran	$4.54 \pm 0.67 \times 10^{-5}$	NA
Dextran with 1 mg/mL AvD	$7.50 \pm 1.97^* \times 10^{-5}$	1.65 ± 0.43
Dextran with 1 mg/mL AvG	$6.46 \pm 1.29^* \times 10^{-5}$	1.42 ± 0.28
PEG	$5.58 \pm 0.53 \times 10^{-6}$	NA
PEG with 1 mg/mL AvD	$5.06 \pm 0.24 \times 10^{-6}$	0.91 ± 0.04
PEG with 1 mg/mL AvG	$5.29 \pm 1.94 \times 10^{-6}$	0.95 ± 0.35

The average \pm SD is reported ($n = 9$). All macromolecules with AvD or AvG were tested for significance against baseline macromolecule transport. Significance is designated. NA, not applicable.

* $P < 0.1$

significantly greater enhancements (fivefold or greater) need to be demonstrated before Avs can be considered as CPEs. One potential avenue for improvement could be increasing the Av concentration and exploring synergistic interactions with other well-established CPEs. Additionally, identifying the skin transport pathway that Avs affect might further help in optimizing their potential as CPEs. Because there is evidence that Avs interact with skin lipids, a more detailed study of how Avs affect the barrier function of skin on long-term and repeated exposure needs to be undertaken. In this context, the inflammatory response to Avs also needs to be studied thoroughly before the potential of Avs in dermatological applications can be realized.

The minimum energy conformation of Avs was estimated using MM2 calculations (Fig. 4), and the structure can be compartmentalized into a central triterpene core, surrounded by tri- and tetrasaccharide side chains. Based on the experimental observations reported here, a possible mechanism for percutaneous transport of Av can be postulated, wherein a combination of the amphiphilic characteristics of the molecule and the presence of an MT-containing side chain may lead to strong interactions with the lipid bilayers. This could potentially result in temporary disruption of the lipid polar head groups. Such disruptions have been shown to occur when MTs interact with lipids (31). In conclusion, the structure of Av provides a potential blue print for the design of molecular transporters and prodrugs for transdermal delivery. In particular, the chemical structures that facilitate the transport of

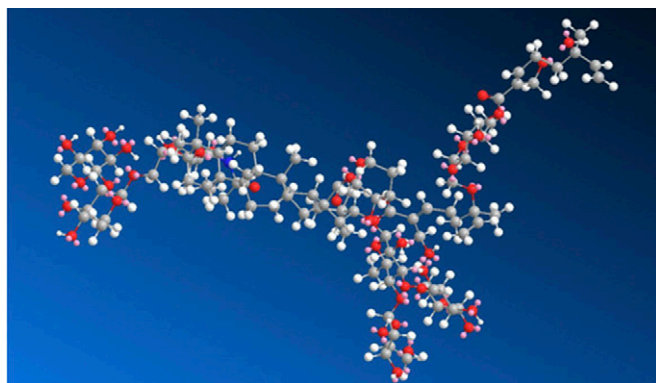


Fig. 4. Three-dimensional atomistic representation of the minimum energy conformation of Avs. The structure was obtained through MM2 calculations and reveals an organization wherein the hydrophilic sugar residues envelope and extend outward from the hydrophobic triterpene core, conferring on it a surfactant-like structure.

Avs could be incorporated in the design of new CPEs and bioactives with self-enhancing transport characteristics.

Materials and Methods

¹²⁵I Radiolabeling of Avs. To determine directly the concentrations of AvD or AvG delivered into and across skin, Avs were labeled with radioactive ¹²⁵I. The choice of the radiolabel was based on the following considerations: (i) ease of labeling and reproducibility; (ii) ¹²⁵I is a high-energy β - and γ -emitter that can be easily measured at low concentrations using a gamma counter or by scintillation and is not labile, unlike tritium; and (iii) more importantly, it adds negligible mass to the Avs in comparison to labeling with fluorophores. Av D and AvG were procured from the Clayton Foundation as white to off-white powder. Briefly, 15 mg of AvD or AvG was dissolved in 150 μ L of DMSO, and the solution was divided into two 75- μ L portions and placed in IodoGen Tubes (Pierce Scientific), which facilitates the iodination reaction. Fifty microliters of ¹²⁵I in the form of NaI (5 mCi, 0.1 mL in NaOH; MPBio) was added to each of the iodination tubes, and the reaction was allowed to proceed for 2 min. The iodinated Av solution was then removed from the IodoGen Tubes and placed into two MacroSpin G-10 silica gel filtration columns (catalog no. SMM S010, molecular mass cutoff of 700 Da; Nest Group). MacroSpin columns were previously prepared by hydrating with distilled deionized (DI) water, allowing for equilibration and then spinning out mobile water. The labeled Av solution was spun at $110 \times g$ for 1 min, and the resulting iodinated solution was free of unreacted NaI and free elemental iodine because both are retained in the size exclusion column. The labeling method as described resulted in the incorporation of about half of the radioactive iodine into the Av molecules (i.e., ~50% labeling efficiency). The final aqueous stock solutions typically had 2.48 mCi and 2.49 mCi of ¹²⁵I activity incorporated in 15 mg of AvD and AvG, respectively. An identical protocol was used for iodination of the AvG fragments as well. For MS analysis, nonradioactive iodine-labeled Avs were used. The location and number of iodine labels on the AvD and AvG and on Av fragments were determined by liquid chromatography (LC)-MS as described below. The degree of iodination, on average, was one iodine per Av molecule, with 44.3% of the iodination occurring at the terminal vinyl group of the outer MT and 37.4% incorporation occurring at the unsaturation in the triterpene core and 18.3% in the tetrasaccharide residue.

Fragmentation of Avs. AvG was used as a model compound for this study and was fragmented using a well-characterized previously described protocol (20). Briefly, Avs were treated with ammonium hydroxide under two different (weak and strong) conditions, yielding different major products. Weak-base treatment involved hydrolysis in 0.5 N of ammonium hydroxide for 1 h at room temperature. Strong-base treatment conditions involved hydrolysis in 1 N of ammonium hydroxide for 18 h at 60 °C. Fragmentation products were thoroughly characterized using LC-MS and concentrated via lyophilization before iodination. The iodination occurred predominantly at the unsaturation in the triterpene core in both the weak-base and strong-base fragments.

Characterization of Iodine-Labeled and Fragmented Avs by LC-MS. Iodinated Avs and fragmentation products of Avs were analyzed by LC-MS with a Thermo Scientific LTQ Mass Spectrometer with a Waters Acquity UPLC LC system equipped with a Hypersil Gold C18 column (2.1 \times 150 mm, 1.9 μ m) using acetonitrile/water as the mobile phase. Exact masses of expected major products were verified with parts per million analysis.

Determination of Radioactivity. The radioactivity was determined using either a Beckman LS6500 beta counter or Perkin-Elmer Packard Tri-Carb 2910TR gamma counter. The receiver solution was transferred into a 10-mL scintillation vial; depending on the measurement, 2 mL or 5 mL of scintillation fluid was added and then counted. Standard curves were established for each radioactive species to ensure that measurements were in the linear range. In the case of ¹²⁵I-labeled Avs, radioactivity was quantified using the gamma counter.

Skin Model and Isolation. Transport and partition studies were carried out using full-thickness pig skin isolated from the dorsal region of adult female pigs (3-mm thickness), which was procured from Lampire Biological Laboratories, and from full-thickness skin isolated from pig ear, respectively. The pig ear skin was isolated as follows. Nonbruised, nonscaled pig (*Sus scrofa domestica*, 4–6 mo old, either sex) ears were obtained from the abattoir (Färber GmbH) within less than 8 h after animals were killed. The ear was rinsed first with cold tap water, hairs were carefully trimmed with clippers,

and full-thickness skin (dorsal portion, ~10 cm × 15 cm, ~1.5-mm thickness) was detached from the underlying cartilage and muscle using a scalpel. The skin was then wrapped in tin foil and stored at -80 °C until further use.

Partition Coefficients. Partition coefficients of Avs and estradiol were measured as described in *SI Materials and Methods*.

Transdermal Transport Studies. Skin was thawed overnight at 5 °C, cut into 1-inch × 1-inch pieces, and mounted in side-by-side glass diffusion cells with an inner diameter of 10 mm (PermeGear), with the SC facing the donor compartment. Both donor and receiver compartments were filled with 2 mL of PBS, and the skin was hydrated for 2 h before experimentation. Skin integrity was verified before and after the transport experiment by measuring an electrical conductance across the skin at 1-kHz, 143.0-mV signal amplitude (33220A Function Generator; Agilent). Skin pieces with conductance values ranging from 8–20 μA at were used in the study. At the commencement of the transport experiments, PBS was removed from the donor compartment and replaced with 2 mL of Avs (0.1 % wt/vol), fragmented Avs (0.1 % wt/vol), or estradiol (saturated solution in PBS with 5 μCi/mL radiolabeled estradiol; Amersham) in PBS and the receiver compartment was filled with fresh PBS. All studies were carried out at ambient temperature (25 °C) and at least in triplicate ($n \geq 3$), using skin from a randomized donor pool of three subjects. This was done to ensure that differences in permeation were not due to donor-to-donor variations. Both the donor and receiver compartments were stirred continuously using microflea stir bars, throughout the duration of the study. At predetermined time points of 3, 6, 12, 18, and 24 h, the solution from the receiver compartment was collected for analysis and replaced with 2 mL of fresh PBS. After the final time point, the integrity of the skin sample was once again verified using electrical measurements.

Permeability was calculated using steady-state transport between 12 and 24 h using the following equation:

$$J = \frac{1}{A} \left(\frac{dM}{dt} \right) = PC_{SS}, \quad [1]$$

where J is steady-state flux ($\mu\text{g}/\text{cm}^2/\text{h}$), A is the cross-sectional area of cell diffusion cell (cm^2), dM/dt is the steady-state transport, P is the permeability ($\text{cm}\cdot\text{h}^{-1}$), and C_{SS} is the concentration of the donor during steady state. C_{SS} was determined as described in *SI Materials and Methods (Determination of the Amount of AvD in the Skin Under Conditions in Which the Donor Concentration Is Held Constant)*. Permeability coefficients for AvD and AvG are reported in Table 1.

- Scheuplein RJ (1976) Percutaneous absorption after twenty-five years: Or "old wine in new wineskins." *J Invest Dermatol* 67(1):31–38.
- Potts RO, Guy RH (1992) Predicting skin permeability. *Pharm Res* 9(5):663–669.
- Mitragotri S (2003) Modeling skin permeability to hydrophilic and hydrophobic solutes based on four permeation pathways. *J Control Release* 86(1):69–92.
- Guy RH, Delgado-Charro MB, Kalia YN (2001) Iontophoretic transport across the skin. *Skin Pharmacol Appl Skin Physiol* 14(Suppl 1):35–40.
- Ogura M, Paliwal S, Mitragotri S (2008) Low-frequency sonophoresis: Current status and future prospects. *Adv Drug Deliv Rev* 60(10):1218–1223.
- Prausnitz MR, Bose VG, Langer R, Weaver JC (1993) Electroporation of mammalian skin: A mechanism to enhance transdermal drug delivery. *Proc Natl Acad Sci USA* 90(22):10504–10508.
- Schramm-Baxter J, Mitragotri S (2004) Needle-free jet injections: dependence of jet penetration and dispersion in the skin on jet power. *J Control Release* 97(3):527–535.
- Prausnitz MR (2004) Microneedles for transdermal drug delivery. *Adv Drug Deliv Rev* 56(5):581–587.
- Karande P, Jain A, Ergun K, Kispersky V, Mitragotri S (2005) Design principles of chemical penetration enhancers for transdermal drug delivery. *Proc Natl Acad Sci USA* 102(13):4688–4693.
- Scheuplein RJ, Blank IH (1971) Permeability of the skin. *Physiol Rev* 51(4):702–747.
- Downing DT (1992) Lipid and protein structures in the permeability barrier of mammalian epidermis. *J Lipid Res* 33(3):301–313.
- Anderson BD, Raykar PV (1989) Solute structure-permeability relationships in human stratum corneum. *J Invest Dermatol* 93(2):280–286.
- Mitragotri S, et al. (2011) Mathematical models of skin permeability: An overview. *Int J Pharm* 418(1):115–129.
- Johnson ME, et al. (1996) Lateral diffusion of small compounds in human stratum corneum and model lipid bilayer systems. *Biophys J* 71(5):2656–2668.
- Rothbard JB, et al. (2000) Conjugation of arginine oligomers to cyclosporin A facilitates topical delivery and inhibition of inflammation. *Nat Med* 6(11):1253–1257.
- Chen Y, et al. (2006) Transdermal protein delivery by a coadministered peptide identified via phage display. *Nat Biotechnol* 24(4):455–460.
- Hsu T, Mitragotri S (2011) Delivery of siRNA and other macromolecules into skin and cells using a peptide enhancer. *Proc Natl Acad Sci USA* 108(38):15816–15821.

Inulin, Dextran, and PEG Transport Studies. ^3H -inulin (MW ~ 5,000, 180 μCi/mg; American Radiolabeled Chemicals), FITC-dextran (MW ~ 3,500, Sigma-Aldrich), and FITC-PEG (MW ~ 3,400, Nanocs) were diluted to the required concentration immediately before use. The donor compartment was filled with a solution containing the permeant (dextran and PEG, 0.1% wt/vol; inulin, 0.002% wt/vol) and 0.1% (wt/vol) AvD or AvG, and the transport studies were carried out as described earlier. Because the objective of this study was simply to evaluate if Avs can facilitate their transport, concentrations identical to an Avs donor concentration of 1 mg/mL were used whenever possible, with the exception of inulin; because these represent concentrations below saturation, it would ensure similar thermodynamic activity for all species. The solution in the receiver compartment was retrieved at 1, 2, 3, 6, 12, 18, and 24 h for analysis and replaced with fresh PBS. In the case of dextran and PEG, a BioTek Synergy-HT fluorescence plate reader was used to determine the mass transported. Fluorescent intensity was determined by exciting at 485 nm and measuring the emission at 520 nm. FITC-dextran and FITC-PEG standards of known concentrations were used to generate linear calibration curves.

DSC of Av-Treated SC. Heat-tripped human SC was punched into a 1.5-cm disks and then incubated overnight in Av solution (1 mg/mL) in a Corning cryovial. Untreated SC subjected to identical conditions served as the control. The SC was then washed and air-dried under ambient conditions. For the DSC analysis, 5–10 mg of the untreated or treated SC was placed in an aluminum DSC pan and crimped, and then immediately placed in the DSC system. DSC curves were obtained using a TA Instrument DSC Q1000 system interfaced to a computer at a heating rate of 10 °C/min over a temperature range of 25–100 °C. A background scan was carried out before each run using empty pans to eliminate any thermal artifacts. The curves were analyzed using the software provided by the manufacturer.

Statistical Analysis. Paired t test analysis was carried out using the statistics module in the Microsoft Excel software package, and $P \leq 0.1$ was considered to be statistically significant because skin exhibits variability.

ACKNOWLEDGMENTS. The authors thank Jeffrey Clanton (Vanderbilt University) for assistance with radiolabeling of the Avs and Av fragments and Dr. Petra Markmeyer-Pieles (University of Freiburg) for help with setting up the radioisotope studies and for providing access to the radioisotope laboratory. This work was supported by grants from the Clayton Foundation for Research (to V.P.S. and J.U.G.). Support through the Excellence Initiative of the German Federal and State Governments Grant EXC 294 (to V.P.S.) is also acknowledged.

- Kumar S, Sahdev P, Perumal O, Tummala H (2012) Identification of a novel skin penetration enhancement peptide by phage display peptide library screening. *Mol Pharm* 9(5):1320–1330.
- Labouta HI, el-Khordagui LK, Kraus T, Schneider M (2011) Mechanism and determinants of nanoparticle penetration through human skin. *Nanoscale* 3(12):4989–4999.
- Jayatilake GS, et al. (2003) Isolation and structures of avicins D and G: In vitro tumor-inhibitory saponins derived from *Acacia victoriae*. *J Nat Prod* 66(6):779–783.
- Samoilov AV, Girshovich ES (1980) [Antibiotic properties of the triterpene glycosides from marine animals of the class Holothuroidea]. *Antibiotiki* 25(4):307–313, Russian.
- Haridas V, et al. (2004) Triterpenoid electrophiles (avicins) activate the innate stress response by redox regulation of a gene battery. *J Clin Invest* 113(1):65–73.
- Haridas V, et al. (2001) Avicins: Triterpenoid saponins from *Acacia victoriae* (Benth) induce apoptosis by mitochondrial perturbation. *Proc Natl Acad Sci USA* 98(10):5821–5826.
- Barbero AM, Frasch HF (2009) Pig and guinea pig skin as surrogates for human in vitro penetration studies: A quantitative review. *Toxicol In Vitro* 23(1):1–13.
- Schmook FP, Meingassner JG, Billich A (2001) Comparison of human skin or epidermis models with human and animal skin in in-vitro percutaneous absorption. *Int J Pharm* 215(1–2):51–56.
- Simon GA, Maibach HI (2000) The pig as an experimental animal model of percutaneous permeation in man: qualitative and quantitative observations—An overview. *Skin Pharmacol Appl Skin Physiol* 13(5):229–234.
- Al-Saidan SM, Barry BW, Williams AC (1998) Differential scanning calorimetry of human and animal stratum corneum membranes. *Int J Pharm* 168(1):17–22.
- Gay CL, Guy RH, Golden GM, Mak VH, Francoeur ML (1994) Characterization of low-temperature (i.e., < 65 degrees C) lipid transitions in human stratum corneum. *J Invest Dermatol* 103(2):233–239.
- Al-Saidan SM (2004) Transdermal self-permeation enhancement of ibuprofen. *J Control Release* 100(2):199–209.
- Griffin S, Wyllie SG, Markham J (1999) Determination of octanol-water partition coefficient for terpenoids using reversed-phase high-performance liquid chromatography. *J Chromatogr A* 864(2):221–228.
- Narishetty ST, Panchagnula R (2004) Transdermal delivery of zidovudine: Effect of terpenes and their mechanism of action. *J Control Release* 95(3):367–379.